Spin coherence in a Mn3 single-molecule magnet

Chathuranga Abeywardana, Andrew M. Mowson, George Christou, and Susumu Takahashi

Citation: Applied Physics Letters **108**, 042401 (2016); doi: 10.1063/1.4940437
View online: http://dx.doi.org/10.1063/1.4940437
View Table of Contents: http://scitation.aip.org/content/aip/journal/apl/108/4?ver=pdfcov
Published by the AIP Publishing

Spin coherence in a Mn_3 single-molecule magnet

Chathuranga Abeywardana,[1] Andrew M. Mowson,[2] George Christou,[2] and Susumu Takahashi[1,3,a)]
[1]*Department of Chemistry, University of Southern California, Los Angeles, California 90089, USA*
[2]*Department of Chemistry, University of Florida, Gainesville, Florida 32611, USA*
[3]*Department of Physics, University of Southern California, Los Angeles, California 90089, USA*

(Received 29 November 2015; accepted 1 January 2016; published online 25 January 2016)

Spin coherence in single crystals of the spin $S = 6$ single-molecule magnet (SMM) $[Mn_3O(O_2CEt)_3(mpko)_3]^+$ (abbreviated Mn_3) has been investigated using 230 GHz electron paramagnetic resonance spectroscopy. Coherence in Mn_3 was uncovered by significantly suppressing dipolar contribution to the decoherence with complete spin polarization of Mn_3 SMMs. The temperature dependence of spin decoherence time (T_2) revealed that the dipolar decoherence is the dominant source of decoherence in Mn_3 and T_2 can be extended up to 267 ns by quenching the dipolar decoherence. © *2016 AIP Publishing LLC*. [http://dx.doi.org/10.1063/1.4940437]

Single-molecule magnets (SMMs) are nanoscale magnets that possess large magnetic moments and an anisotropy energy barrier between their spin-up and spin-down states at the molecular level. The energy barrier prevents spin reversal, leading to slow magnetization relaxation and hysteresis (bistability) at low temperatures.[1,2] The quantum mechanical nature of their nanomagnetism also emerges at low temperatures, with behaviors such as quantum tunneling of magnetization (QTM)[3–5] and quantum phase interference of two tunneling paths (Berry phase).[6–8] Various types of SMMs with different sizes of magnetic moments and energy barriers have been synthesized, including SMMs made from several transition metal ions,[1,2,9–14] a dimer of SMMs,[15,16] and mononuclear SMMs based on lanthanides.[17–20] The nanomagnetism and spin physics of SMMs have been extensively investigated on large ensembles of SMMs.[1–6,21–23] In addition, it has been demonstrated that an individual SMM or a small ensemble of SMMs can be placed on a surface with some retention of their magnetic behavior;[24–30] therefore, SMMs are also candidates for potential applications in dense quantum memory, quantum computing, and molecular spintronics.[29,31,32]

In spite of wide interest in the quantum nature of SMMs, decoherence effects that ultimately limit such behavior have yet to be fully understood. Until now, coherent manipulation of spin states in SMMs has been experimentally demonstrated only in a very few cases, including Fe_8,[33,34] V_{15},[35] Fe_4,[36] and Cr_7M (M = Ni and Mn)[37] systems. In particular, even though Mn-based SMMs have been extensively studied for over two decades, no coherent manipulation on Mn-based SMMs has been reported to date. Recent investigations have shown that there are three main decoherence mechanisms present in SMMs: spins can couple locally (1) to phonons (phonon decoherence); (2) to many nuclear spins (nuclear decoherence); and (3) to each other via dipolar interactions (dipolar decoherence).[33,38,39] In particular, the long-range nature of dipolar interactions is a major problem in many SMMs. Interestingly, recent experimental investigations have demonstrated that dipolar decoherence is significantly suppressed using high-frequency electron paramagnetic resonance (HF-EPR) spectroscopy at low temperature.[33,34,40]

In this paper, we investigate spin coherence in single crystals of the SMM $[Mn_3O(O_2CEt)_3(mpko)_3](ClO_4)$, abbreviated Mn_3, which has a ground state spin of $S = 6$.[41,42] In addition, quantum mechanical couplings between different

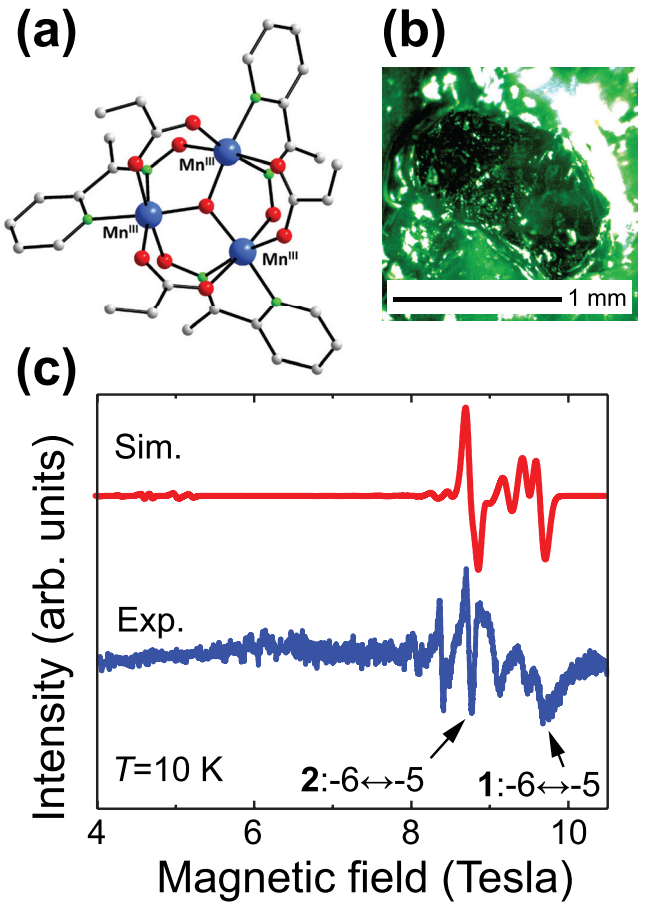

FIG. 1. (a) A schematic of the structure of Mn_3. (b) A photo of sample A. (c) 230 GHz EPR cw spectrum of Mn_3. The $m_S = -6 \leftrightarrow -5$ transitions from each orientation are indicated by arrows (labeled **1** and **2**). In the simulation, $\theta = 75°$ and $\phi = 0°$ for group **1** and $\theta = 69°$ and $\phi = 74°$ for group **2**, where θ and ϕ are azimuthal and polar angles of the molecular axis, respectively ($\mathbf{B_0}$ is along the z-axis).

a)Electronic mail: susumu.takahashi@usc.edu

Mn_3 SMMs have recently been demonstrated with synthesis of a covalently linked dimer[43] and tetramer[44] while retaining the intrinsic magnetic properties of each Mn_3 SMM. Therefore, the Mn_3 system is clearly a potentially great testbed for investigating quantum coherence in Mn-based SMMs. The investigation was performed with continuous-wave (cw) and pulsed EPR spectroscopy at 230 GHz. Using 230 GHz cw EPR spectroscopy, we first identified the EPR transition between the $m_S = -6$ and $m_S = -5$ states, and then performed spin echo measurements to probe the coherence in Mn_3 SMMs. At resonance, the energy difference between the $m_S = -6$ and $m_S = -5$ states is 11 K, so Mn_3 spins are almost completely polarized to the $m_S = -6$ ground state below 2.0 K. This complete polarization significantly reduces the dipolar decoherence. At 1.6 K, the spin decoherence time (T_2) of Mn_3 was measured to be 205 ns. Upon raising the temperature to 2.2 K, the T_2 decreased by nearly one order of magnitude. As temperature increases, so do magnetic fluctuations caused by the magnetic dipole interaction between SMMs; thus, T_2 is reduced. An excellent agreement between the observed temperature dependence of T_2 and the dipolar decoherence model strongly supports that a major source of the spin decoherence is dipolar decoherence. In addition, we will show that there exist other decoherence sources which limit the maximum T_2 to be 260 ns.

The Mn_3 SMM consists of three Mn^{III} atoms each with spin $S = 2$. These are ferromagnetically coupled to each other to give the total spin of $S = 6$. A schematic of the molecular structure is shown in Figure 1(a). The following Hamiltonian is sufficient to describe the magnetic properties of Mn_3 SMMs

$$H = \mu_B g \mathbf{S} \cdot \mathbf{B}_0 + DS_z^2 + E(S_x^2 - S_y^2). \quad (1)$$

The first term of the Hamiltonian (Equation (1)) is the electronic Zeeman interaction, where μ_B is the Bohr magneton, g is the isotropic g-factor which equals assume to be 2.00, $\mathbf{S}$ is the spin operator, and $\mathbf{B_0}$ is the applied magnetic field. The second and third terms represent zero-field interaction terms corresponding to axial and rhombic anisotropies, which are $D = -10$ GHz and $E = 0.3$ GHz, respectively.[41] Higher order terms in the spin Hamiltonian have been excluded in this study. It is important to note that having a large negative D-value and a high spin quantum number ($S = 6$) leads to large zero-field splittings within Mn_3 (110 GHz for the $m_S = -6$ and -5 states). In addition, it has been shown in previous studies that a single crystal of Mn_3 consists of two spin sub-groups where the easy axes of each group are oriented with an angle of $\sim 70°$.[41]

In the present study, two single crystals of Mn_3 SMMs were investigated (called here samples A and B) using a 230 GHz cw and pulsed EPR spectroscopies. The 230 GHz EPR spectrometer is based on a 100 mW solid-state source, quasi-optics, a superheterodyne detection system, and a 12.1 T superconducting magnet. Details of this spectrometer can be found elsewhere.[45] Both crystals were slab-shaped (see Figure 1(b) for sample A) and placed on a conducting end-plate in the sample holder where the orientation of the

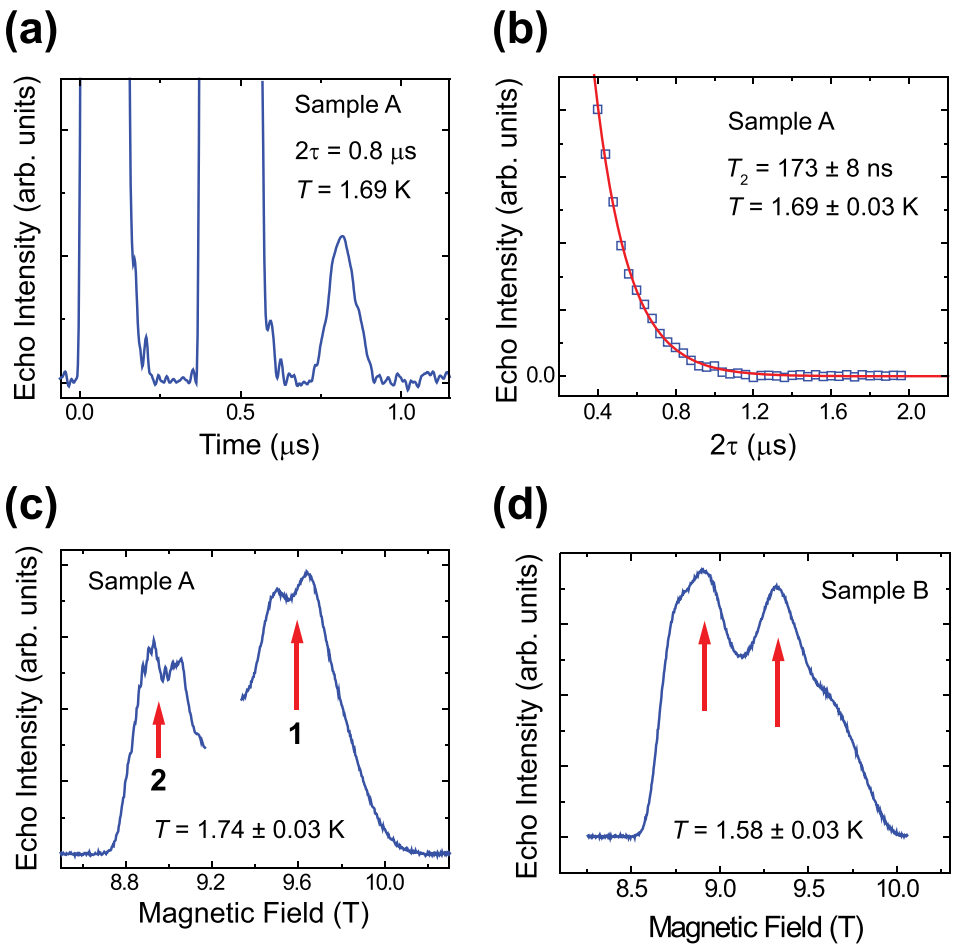

FIG. 2. Spin echo measurements of Mn_3 crystals. (a) The echo signal at 1.69 K. The optimal pulse widths in the spin echo sequence were found to be $\pi/2 = 60$ ns and $\pi = 90$ ns by adjusting the pulse length to maximize the echo intensity. Shown pulse widths are highly exaggerated due to the free induction decay (FID). This snapshot of the oscilloscope trace was taken at $2\tau = 800$ ns. The signal was averaged 16 times. (b) Spin echo decay at 1.69 K. Intensity of the echo peak plotted as a function of 2τ. Data were fitted by a single exponential and T_2 was extracted as 173 ns. (c) EDFS data from sample A. Spin echo intensity at $2\tau = 700$ ns recorded as magnetic field sweeps. For this measurement, $\pi/2$ and π pulses were 100 ns and 150 ns, respectively. The $m_S = -6 \leftrightarrow -5$ transitions are labeled by arrows. (d) EDFS data from sample B. Spin echo intensity at $2\tau = 500$ ns recorded as magnetic field sweeps. For this measurement, $\pi/2$ and π pulses were 80 ns and 100 ns, respectively. The $m_S = -6 \leftrightarrow -5$ transitions are labeled by arrows.

external magnetic field (B_0) is perpendicular to the crystal plane. Figure 1(c) shows a 230 GHz cw EPR spectrum taken at 10 K. The applied microwave excitation power and the field modulation intensities were carefully tuned to prevent distortions in the EPR lineshape. As shown in Figure 1(c), the simulated EPR spectrum using Equation (1) agrees fairly well with the experimental spectrum. The two EPR signals at 9.6 T and 8.9 T (labeled as **1** and **2**) originate from the $m_S = -6 \leftrightarrow -5$ transition of the two different spin groups in the Mn_3 crystal.

Next, we investigated spin decoherence in Mn_3 using 230 GHz pulsed EPR spectroscopy. For the measurement, the magnetic field was first set to 9.6 T, which corresponds to the $m_S = -6 \leftrightarrow -5$ transition of Group **1**, as shown in Figure 1(c), then we applied the spin echo sequence ($\pi/2$-τ-π-τ-echo) where τ is the free evolution time of spins. As shown in Figure 2(a), the echo signal was clearly observed at $2\tau = 0.8\,\mu$s, which confirms the detection of coherence in a Mn-based SMM. In addition, we measured the echo intensity as a function of 2τ to determine the spin decoherence time (T_2). As shown in Figure 2(b), the observed decay of the echo intensity was well represented by a single exponential function. We therefore extracted the spin decoherence time (T_2) to be 173 ns by fitting the decay to the single exponential function ($\exp(-2\tau/T_2)$). Echo-detected field sweep (EDFS) measurements were also performed by measuring the echo intensity as a function of magnetic field to verify the EPR transitions. Figure 2(c) shows EDFS measurements taken at 1.74 K. As shown in Figure 2(c), two pronounced peaks were observed at 9.6 T and 8.9 T (labeled **1** and **2**, respectively) for sample A, which are consistent with the $m_S = -6 \leftrightarrow -5$ transitions. Similarly, we observed two pronounced EDFS signals from sample B, as shown in Figure 2(d).

Finally, in order to identify the major sources of spin decoherence in Mn_3, we studied T_2 as a function of temperature. As shown in Figure 3(a), T_2 at 1.58 K was measured to be 205 ± 6 ns for sample A, then T_2 decreases rapidly as the temperature was increased. T_2 was extracted up to 2.2 K ($T_2 = 59 \pm 30$ ns). Above 2.2 K, T_2 became too short to measure due to the limitation in the time resolution of the EPR spectrometer. The temperature dependence of T_2 is summarized in Figure 3(a). At low temperature ($k_B T \ll h\nu_{Larmor}$, where k_B is the Boltzmann constant and T is temperature), the dipolar decoherence is caused by the interaction between the $k = 0$ magnon, which is excited by the microwave excitation, and a thermally excited magnon ($k \neq 0$ magnon); therefore, the decoherence rate ($1/T_2$) is highly dependent on the population of the thermally excited magnon. At 230 GHz and such low temperatures, the Mn_3 polarization is above 99%, which almost eliminates the thermally excited magnon. Using the previously reported model,[33,38] the temperature dependence of the decoherence rate ($1/T_2$) is given by

$$1/T_2 = A \exp\left(-h\nu_{Larmor}/k_B T\right) + \Gamma, \qquad (2)$$

where the first term is the dipolar decoherence rate, A is a constant, and the second term is the residual decoherence rate, i.e., phonon and nuclear decoherence. As shown in Figure 3(b), a fit of the temperature dependence to Equation (2) agrees well, and the analysis indicates that the dipolar

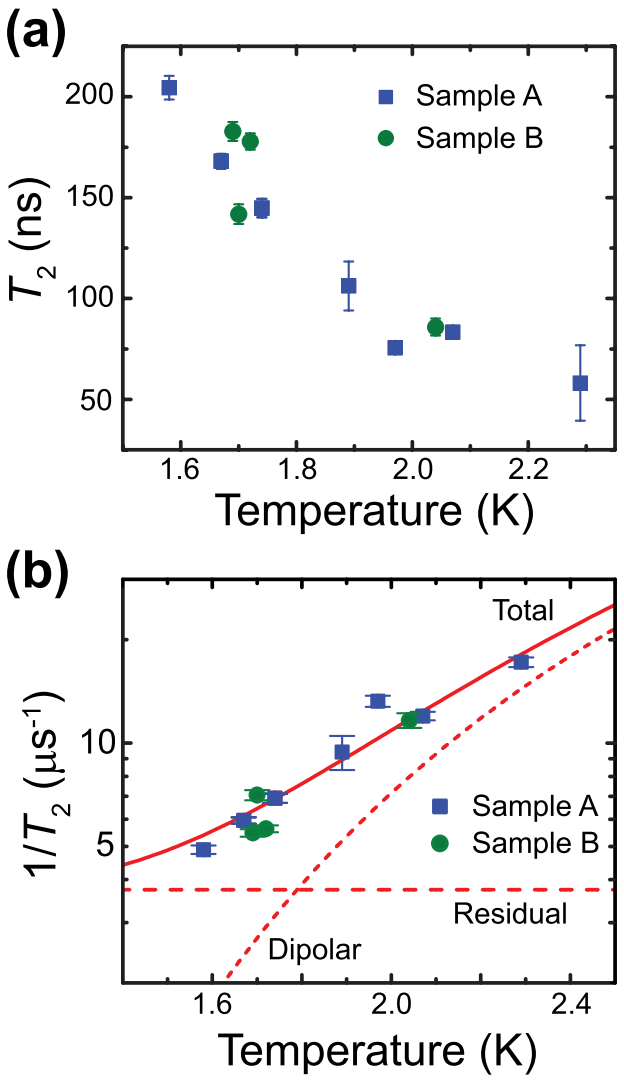

FIG. 3. Temperature dependence of the spin decoherence for samples A and B. (a) Spin decoherence time (T_2) as a function of temperature. The measurements were performed at 9.6 T and 8.9 T for samples A and B, respectively. (b) The rate of spin decoherence as a function of temperature. The long-dashed line shows the contribution to spin decoherence from the residual decoherence sources, whereas the short-dashed line denotes the dipolar contribution. The solid line shows the total decoherence from these two contributions.

decoherence is dominant in the higher temperature regime. The obtained value of A is $1785 \pm 149\,\mu s^{-1}$. It is important to note that a similar strength of the dipolar decoherence was found in a single crystal of Fe_8 SMMs ($A \sim 3000\,\mu s^{-1}$).[33] On the other hand, the decoherence is limited by the residual source at low temperatures. The amount of the residual decoherence determines the magnitude of the spin decoherence time by quenching the dipolar decoherence. As shown in Figure 3(b), we obtained 267 ± 36 ns for the residual decoherence time ($1/\Gamma$).

In summary, we have investigated spin coherence in Mn_3 SMMs. Using the HF-EPR spectroscopy, we revealed coherence in Mn_3 SMMs by suppressing the dipolar decoherence. In addition, temperature dependence of T_2 showed that the dominant source of the decoherence is the dipolar decoherence and the decoherence time can be extended to 267 ns by quenching the dipolar decoherence.

This work was supported by the National Science Foundation (DMR-1508661, S.T.; DMR-1213030, G.C.) and the Searle Scholars Program (S.T.).

[1]D. Gatteschi, R. Sessoli, and J. Villain, *Molecular Nanomagnets* (Oxford University Press, New York, 2006).
[2]G. Christou, D. Gatteschi, D. N. Hendrickson, and R. Sessoli, MRS Bull. **25**, 66 (2000).
[3]J. R. Friedman, M. P. Sarachik, J. Tejada, and R. Ziolo, Phys. Rev. Lett. **76**, 3830–3833 (1996).
[4]L. Thomas, Nature **383**, 145–147 (1996).
[5]C. Sangregorio, T. Ohm, C. Paulsen, R. Sessoli, and D. Gatteschi, Phys. Rev. Lett. **78**, 4645–4648 (1997).
[6]W. Wernsdorfer and R. Sessoli, Science **284**, 133–135 (1999).
[7]C. M. Ramsey, E. del Barco, S. Hill, S. J. Shah, C. C. Beedle, and D. N. Hendrickson, Nat. Phys. **4**, 277–281 (2008).
[8]H. M. Quddusi, J. Liu, S. Singh, K. J. Heroux, E. del Barco, S. Hill, and D. N. Hendrickson, Phys. Rev. Lett. **106**, 227201 (2011).
[9]A. Caneschi, D. Gatteschi, R. Sessoli, A. L. Barra, L.-C. Brunel, and M. Guillot, J. Am. Chem. Soc. **113**, 5873–5874 (1991).
[10]K. Wieghardt, K. Pohl, I. Jibril, and G. Huttner, Angew. Chem. Int. Ed. Engl. **23**, 77–78 (1984).
[11]E. del Barco, A. Kent, E.-C. Yang, and D. N. Hendrickson, Phys. Rev. Lett. **93**, 157202 (2004).
[12]D. Gatteschi, L. Pardi, A. L. Barra, and A. Mueller, Nature **354**, 463–465 (1991).
[13]D. Gatteschi, R. Sessoli, and A. Cornia, Chem. Commun. **2000**, 725–732 (2000).
[14]D. Gatteschi, A. Caneschi, L. Pardi, and R. Sessoli, Science **265**, 1054–1058 (1994).
[15]W. Wernsdorfer, N. Aliaga-Alcalde, D. N. Hendrickson, and G. Christou, Nature **416**, 406–409 (2002).
[16]S. Hill, R. S. Edwards, N. Aliaga-Alcalde, and G. Christou, Science **302**, 1015–1018 (2003).
[17]N. Ishikawa, M. Sugita, T. Ishikawa, S. Koshihara, and Y. Kaizu, J. Am. Chem. Soc. **125**, 8694–8695 (2003).
[18]R. Sessoli and A. K. Powell, Coord. Chem. Rev. **253**, 2328–2341 (2009).
[19]J. D. Rinehart and J. R. Long, Chem. Sci. **2**, 2078–2085 (2011).
[20]L. Sorace, C. Benelli, and D. Gatteschi, Chem. Soc. Rev. **40**, 3092–3104 (2011).
[21]Y. Suzuki, M. P. Sarachik, E. M. Chudnovsky, S. McHugh, R. Gonzalez-Rubio, N. Avraham, Y. Myasoedov, E. Zeldov, H. Shtrikman, N. E. Chakov, and G. Christou, Phys. Rev. Lett. **95**, 147201 (2005).
[22]M. Martens, J. V. Tol, N. S. Dalal, S. Bertaina, B. Barbara, B. Tsukerblat, A. Müller, S. Garai, S. Miyashita, and I. Chiorescu, Phys. Rev. B **89**, 195439 (2014).
[23]E. del Barco, A. D. Kent, S. Hill, J. M. North, N. S. Dalal, E. M. Rumberger, and D. N. Hendrickson, J. Low Temp. Phys. **140**, 119–174 (2005).
[24]M. Mannini, F. Bertani, C. Tudisco, L. Malavolti, L. Poggini, K. Misztal, D. Menozzi, A. Motta, E. Otero, P. Ohresser, P. Sainctavit, G. G. Condorelli, E. Dalcanale, and R. Sessoli, Nat. Commun. **5**, 4582 (2014).
[25]M.-H. Jo, J. E. Grose, K. Baheti, M. M. Deshmukh, J. J. Sokol, E. M. Rumberger, D. N. Hendrickson, J. R. Long, H. Park, and D. C. Ralph, Nano Lett. **6**, 2014–2020 (2006).
[26]H. B. Heersche, Z. D. Groot, J. A. Folk, H. S. J. V. D. Zant, C. Romeike, M. R. Wegewijs, L. Zobbi, D. Barreca, E. Tondello, and A. Cornia, Phys. Rev. Lett. **96**, 206801 (2006).
[27]R. Vincent, S. Klyatskaya, M. Ruben, W. Wernsdorfer, and F. Balestro, Nature **488**, 357–360 (2012).
[28]M. Mannini, F. Pineider, P. Sainctavit, C. Danieli, E. Otero, C. Sciancalepore, A. M. Talarico, M.-A. Arrio, A. Cornia, D. Gatteschi, and R. Sessoli, Nat. Mater. **8**, 194–197 (2009).
[29]M. Urdampilleta, S. Klyatskaya, J.-P. Cleuziou, M. Ruben, and W. Wernsdorfer, Nat. Mater. **10**, 502–506 (2011).
[30]J. J. Henderson, C. M. Ramsey, E. del Barco, A. Mishra, and G. Christou, J. Appl. Phys. **101**, 09E102 (2007).
[31]M. N. Leuenberger and D. Loss, Nature **410**, 789–793 (2001).
[32]L. Bogani and W. Wernsdorfer, Nat. Mater. **7**, 179–186 (2008).
[33]S. Takahashi, I. S. Tupitsyn, J. van Tol, C. C. Beedle, D. N. Hendrickson, and P. C. E. Stamp, Nature **476**(7358), 76–79 (2011).
[34]S. Takahashi, J. van Tol, C. C. Beedle, D. N. Hendrickson, L.-C. Brunel, and M. S. Sherwin, Phys. Rev. Lett. **102**, 087603 (2009).
[35]S. Bertaina, S. Gambarelli, T. Mitra, B. Tsukerblat, A. Muller, and B. Barbara, Nature **453**, 203–206 (2008).
[36]C. Schlegel, J. V. Slageren, M. Manoli, E. K. Brechin, and M. Dressel, Phys. Rev. Lett. **101**, 147203 (2008).
[37]A. Ardavan, O. Rival, J. J. L. Morton, S. J. Blundell, A. M. Tyryshkin, G. A. Timco, and R. E. P. Winpenny, Phys. Rev. Lett. **98**, 057201 (2007).
[38]A. Morello, P. C. E. Stamp, and I. S. Tupitsyn, Phys. Rev. Lett. **97**, 207206 (2006).
[39]P. C. E. Stamp and I. S. Tupitsyn, Phys. Rev. B **69**, 014401 (2004).
[40]S. Takahashi, R. Hanson, J. van Tol, M. S. Sherwin, and D. D. Awschalom, Phys. Rev. Lett. **101**(4), 047601 (2008).
[41]T. C. Stamatatos, D. Foguet-Albiol, S.-C. Lee, C. C. Stoumpos, C. P. Raptopoulou, A. Terzis, W. Wernsdorfer, S. O. Hill, S. P. Perlepes, and G. Christou, J. Am. Chem. Soc. **129**, 9484–9499 (2007).
[42]T. C. Stamatatos, D. Foguet-Albiol, C. C. Stoumpos, C. P. Raptopoulou, A. Terzis, W. Wernsdorfer, S. P. Perlepes, and G. Christou, J. Am. Chem. Soc. **127**, 15380–15381 (2005).
[43]T. N. Nguyen, M. Shiddiq, T. Ghosh, K. A. Abboud, S. Hill, and G. Christou, J. Am. Chem. Soc. **137**, 7160–7168 (2015).
[44]T. N. Nguyen, W. Wernsdorfer, K. A. Abboud, and G. Christou, J. Am. Chem. Soc. **133**, 20688–20691 (2011).
[45]F. H. Cho, V. Stepanov, and S. Takahashi, Rev. Sci. Instrum. **85**, 075110 (2014).